Research Square

Preprints are preliminary reports that have not undergone peer review.
They should not be considered conclusive, used to inform clinical practice,
or referenced by the media as validated information.

Optimal Photon Energy Transfer on Titanium Targets for Laser Thrusters

Aurelian Marcu (aurelian.marcu@inflpr.ro)
National Institute for Laser Plasma and Radiation Physics
Mihai Stafe
Polytechnic University of Bucharest
Barbuta Mihail-Gabriel
Polytechnic University of Bucharest
Ungureanu Razvan
National Institute for Laser Plasma and Radiation Physics
Mihai Serbanescu
National Institute for Laser Plasma and Radiation Physics
Bogdan Calin
National Institute for Laser Plasma and Radiation Physics
Puscas Nicolae
Polytechnic University of Bucharest

Research Article

Keywords: infrared pulsed lasers systems, TEWALASS , CETAL-NILPRP, optimal laser

Posted Date: May 11th, 2021

DOI: https://doi.org/10.21203/rs.3.rs-504102/v1

License: This work is licensed under a Creative Commons Attribution 4.0 International License.
Read Full License

Optimal photon energy transfer on titanium targets for laser thrusters

Marcu A[1,*], Stafe M[2,*], Barbuta M[2], Ungureanu R[1], Serbanescu M[1], Calin B[1], and Puscas N[2]

[1]Center for Advanced Laser Technologies (CETAL), National Institute for Laser, Plasma and Radiation Physics (INFLPR), 409 Atomistilor, Magurele, 077125, Romania
[2]Department of Physics, University Politehnica of Bucharest, Splaiul Independentei 313, Bucharest, 060042, Romania
[*]aurelian.marcu@inflpr.ro
[*]mihai.stafe@physics.pub.ro

ABSTRACT

Using two infrared pulsed lasers systems: a picosecond solid-state Nd:YAG laser with tunable repetition rate (400 kHz - 1 MHz) working in a burst mode of multi-pulse train and a femtosecond Ti:Sapphire laser amplifier with tunable pulse duration in the range of tens of femtoseconds up to tens of picoseconds, working in single-shot mode (TEWALASS facility from CETAL-NILPRP), we have investigated the optimal laser parameters for kinetic energy transfer to a titanium target for laser-thrust applications. In the single-pulse regime, we controlled the power density by changing both duration and pulse energy. In the multi-pulse regime, the train's number of pulses (burst length), and the pulse energy variation were investigated. Heat propagation and photon reflection-based models were used to simulate obtained experimental results. In the single-pulse regime, optimal kinetic energy transfer was obtained for power densities of about 500 times the ablation threshold corresponding to the specific laser pulse duration. In multi-pulse regimes, the optimal number of pulses per train increases with the train frequency and decreases with the pulse power density. An ideal energy transfer efficiency resulting from our experiments and simulations is close to around 0.02%.

Introduction

Laser-matter interaction is a rather complex process representing a broad research domain with numerous scientific and technology applications in various domains of activities: from engineering and nanotechnology to medicine or astronomy[1–3]. Photon is known as a mass-less particle in the quantum physics approach, but still able to transfer impulse and respectively kinetic energy to macroscopic targets ($E_p = h_{Planck} * \nu$). Because the Planck constant h_{Planck} has a very small value of about 10^{-34} m^2kg/s, transferred energy has usually a neglectable value at the macroscopic scale, but, since the total transferred energy depends on the total number of photons and photon associated frequency, there are cases, and consequently, applications, where this energy is no longer neglectable. Transferred impulse and respectively kinetic energy while irradiating, started to be experimentally measured from the beginning of the 20th century based on the Maxwell theoretical model and later studied for laser-thrust possible applications[4–7]. More recent applications based on ultra-intense laser pulse light radiation pressure were developed in the field of particle acceleration such as ions[8] to relativistic energies, using ultra-intense laser pulses. According to the theory, if the laser peak power density (intensity) exceeds values of 10^{24} W/cm^2 on a target thicker than several atomic layers, after being fully ionized it will act as a plasma mirror that will reflect the incident pulse, taking a significant amount of its impulse[9]. It is known that kinetic energy transfer efficiency depends on several parameters like laser wavelength, target material, but, for a given target material and a particular laser beam it mostly depends on the beam power density on the target[10]. However, in a pulsed laser system, the power density can be changed by controlling three main parameters, pulse energy, beam size, or pulse duration. Since for real applications changing the beam size (respectively changing the focus position while following a moving target) is not always a practical solution, studies usually address the other two ways: controlling pulse energy and respectively pulse duration. While the existing experimental studies on light pulse kinetic energy transfer to targets are performed on rather limited power range intervals – usually obtained by varying only the pulse energy – corroborated studies on wider ranges mostly rely on combined individual studies performed with rather different lasers wavelengths, pulse duration, and target material[7]. In terms of pulse duration, previous studies have shown that for long laser pulses (e.g. ns or longer), the dissipation of the absorbed energy in the bulk material and possibly material removal takes place during the laser pulse duration[11]. For pulses shorter than the characteristic relaxation times (e.g. below few ps) during the laser-matter

interaction process, the photon energy will be transferred to the electrons and they will further transfer it to the target atoms as electron-to-ion energy transfer. All of these processes typically occur on the order of several picoseconds after laser absorption. Hence, for short laser pulses, heat diffusion is confined during the interaction of the laser beam with material and the shock-like energy transfer leads to ablation. Thus, there should be significant differences between controlling the power density by energy or by pulse duration. In the present work, we start with a systematic study in single-shot mode on the correlation between the laser pulse power density and the efficiency of kinetic energy transfer for a given target (titanium in our case) with fixed geometry using an infrared pulsed laser beam (Ti:Sapphire CPA laser amplifier at TEWALAS facility part of CETAL INFLPR). For this purpose, we have varied the pulse duration while maintaining the pulse energy and vice versa. Because in a propulsion application, more pulses (train of pulses) should be more likely needed, we have further investigated the influence of the number of pulses, repetition rate, and energy per pulse over the kinetic energy transfer within the range of our experimental tools of 1 MHz repetition rate. For a deeper understanding of the obtained data and processes, the experimental results were compared with computer simulations of photo-thermal induced effect models[11–15] with similar (or comparable) laser-target interaction parameters.

Results and discussions

Impulse transfer experimental measurements were initially performed on the titanium target for pulses with 7 ps duration and train energies W_{train} = 426 mJ and 652 mJ, and variable repetition rate f_p between 400 kHz and 1000 kHz. By changing the number of pulses N within a train while keeping the train energy W_{train} and duration constant we have also changed 'effective' laser-target interaction duration and respectively pulse power density and the result was a change in the kinetic energy efficiency transfer as presented in Figure 1a. These results could be considered 'predictable' as long as the laser-thrust efficiency is known to increase with the laser power density[10]. Power density variation in the domain of 10^{11} W/cm^2 - 10^{13} W/cm^2 was further investigated also by adjusting the laser-mater interaction duration at 30 mJ and 70 mJ single pulse constant energies but the resulting trend is an opposite one in this case as presented in Figure 1b. Considering the different trends over kinetic energy transfer efficiency for power variations obtained with similar methods (reducing the laser-matter interaction time at constant energies), there is obvious evidence that it should be an 'optimal' power density in between the two power ranges, corresponding to specific pulse duration and energy for a maximal kinetic energy transfer efficiency as also previously mentioned in other publications[5,6].

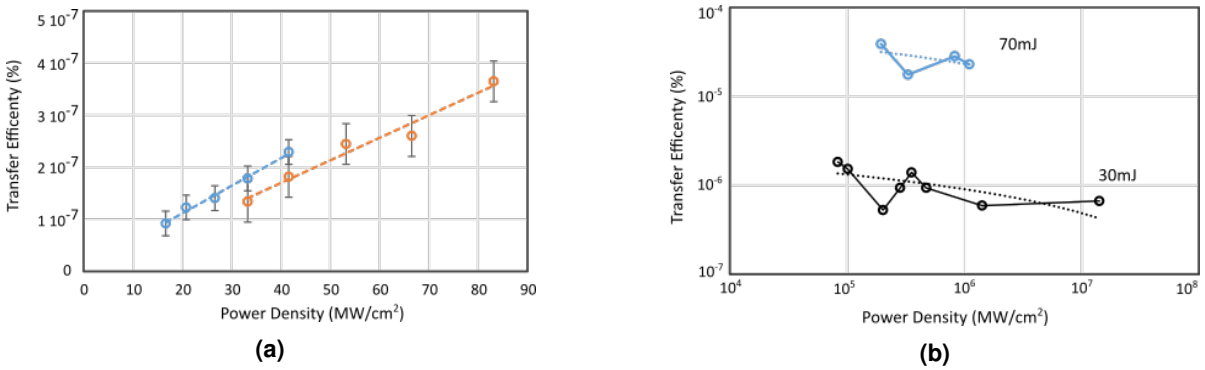

Figure 1. Kinetic energy transfer efficiency at different beam energies for (a) multi-pulse ps laser (tuned train frequency) and (b) single pulse fs laser (with tuned duration)

Single-pulse regime: Optimal pulse duration

For understanding the above-presented results we started by modeling single-pulse laser-matter interaction experimental results and numerical results on the dependence of transfer efficiency on the pulse duration and pulse power density, at several constant pulse energies, are presented in Figure 2. The laser power density was varied by setting the pulse energy constant (W_p = 10, 30, 50, 70, 90, 110 mJ) and changing the pulse duration in the range of 1 µs - 1 ps. Thus, simulations suggest that for fixed pulse energy, the transfer efficiency is very small and constant at a long pulse duration of the order of 1 - 10 µs or even more depending on pulse energy. Further decrease of the pulse duration sets in the ablation process and the strong recoil pressure of the ablation plume are leading to about 6 to 8 orders of magnitude increase of the transfer efficiency. It should be noticed that the transfer efficiency and the optimal pulse duration are both dependent on the pulse power density, as shown by simulation results presented in Figure 2b which are in good agreement with the experimental data. The results presented in Figure 2a indicate that the optimal pulse duration is of the order of a few ps for W_p = 10 mJ, and an increase of pulse energy above W_p =

100 mJ leads to an optimal pulse duration of a few hundreds of ps. Figure 2b indicates a limit value for the transfer efficiency of about 10^{-3}% for laser power density of about ≈ 5 GW/cm^2. It should be also noticed from Figure 2b that the ratio of the optimal laser power density to the ablation threshold power density is approximately 500:1 for the pulse energies considered here. This correlation relies on the competition between enhancement of the recoil pressure with laser power density, and the enhancement of the plume absorptivity with laser power density since both processes dominate over the radiation pressure mechanism above the ablation threshold.

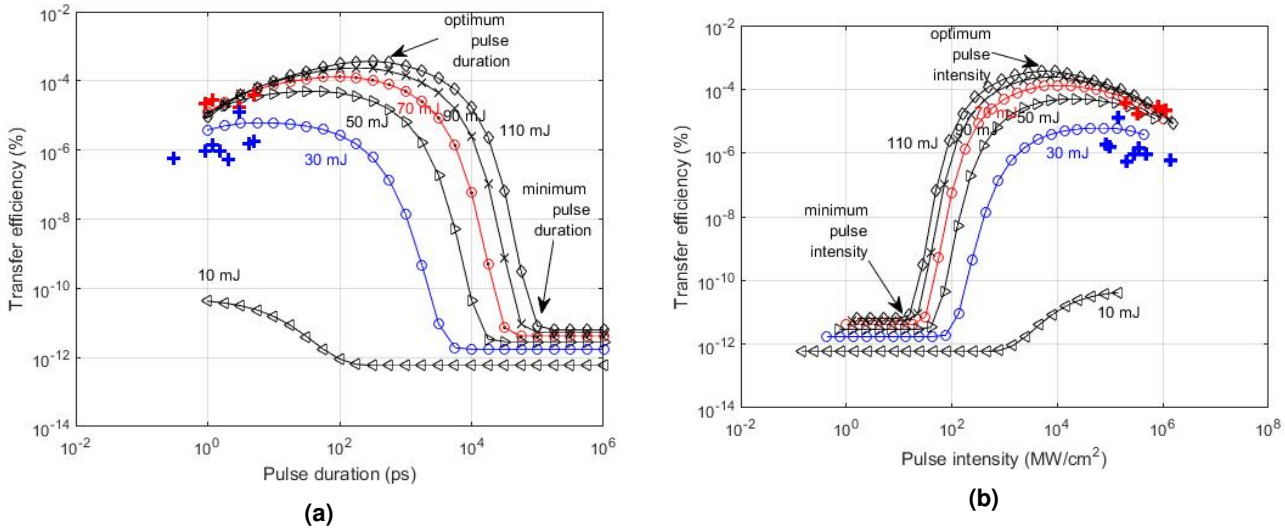

Figure 2. Kinetic energy efficiency transfer, dependence on (a) pulse duration and (b) power density. Experimental data are represented as blue (W_p = 30 mJ) and red (W_p = 70 mJ) crosses.

Single-pulse regime: Optimal pulse energy

In most of the real experimental cases, the laser pulse duration is actually the system's constant value rather than the pulse energy. We started from the fact that even if at power densities of the order 10^{12} W/cm^2 where the increase is based on the pulse duration reduction, the efficiency of the kinetic energy transfer is decreasing, an increase of the power density based on the increase of the pulse energy in a certain range (up to few times in our case) is giving an opposite trend as shown in Figure 3a for a single laser pulse with duration estimated at 35 fs and pulse energy up to about 120 mJ in our particular case. It is evident that with the increase of the pulse energy for fixed pulse duration, transfer efficiency increases less and less, and after a value which in our experimental case (for a 35 fs duration and titanium target material) is about 4 × 10^{13} W/cm^2, kinetic energy transfer efficiency starts to decrease. In other words, the increase of the pulse energy should increase the transfer efficiency just within a limited interval. Further experiments performed at different pulse durations within the picoseconds scale range have confirmed the efficiency transfer increasing trend, but, with a power density (and respectively pulse duration) slope dependence on power density. Thus, Figure 3b presents the influence of pulse energy increase from 30 mJ to 70 mJ for different laser pulse durations. In all cases, we are having an increase in the transfer efficiency, but the slope is gradually decreasing with the decrease of the pulse duration and respectively with the increase of the power density, as represented in the inset of Figure 3b.

Numerical simulations of transfer efficiency dependence on the pulse energy at constant pulse duration were represented in Figure 4a. They suggest that, in fact, the kinetic energy transfer efficiency does not significantly depend on pulse duration at small pulse energies, corresponding to power densities below the ablation threshold. At higher power densities above the ablation threshold (and respectively shorter pulse duration), the efficiency could reach one-two orders of magnitude higher values for longer pulses (i.e. 5.1 ps duration) as compared to short pulse duration (3 ps and 1.2 ps respectively) supporting the experimental efficiency variation trend previously presented. In terms of power density variation (controlled by pulse energy variation at constant pulse duration), Figure 4b shows a very small transfer efficiency value, increasing linearly with pulse power density when the laser power density is below the ablation threshold. For further increase of power density, above the ablation threshold, strong recoil pressure of the ablation plume leads to a magnitude increase up to 8 orders of the transfer efficiency, in good agreement with the (bold circles from Figure 4b) experimental results. Even if the optimal pulse energy depends on the pulse duration for our experimental conditions, with the increase of the pulse energy there is still an about 500:1 ratio between the optimal power density and the ablation threshold. For our investigated experimental case, simulations suggest

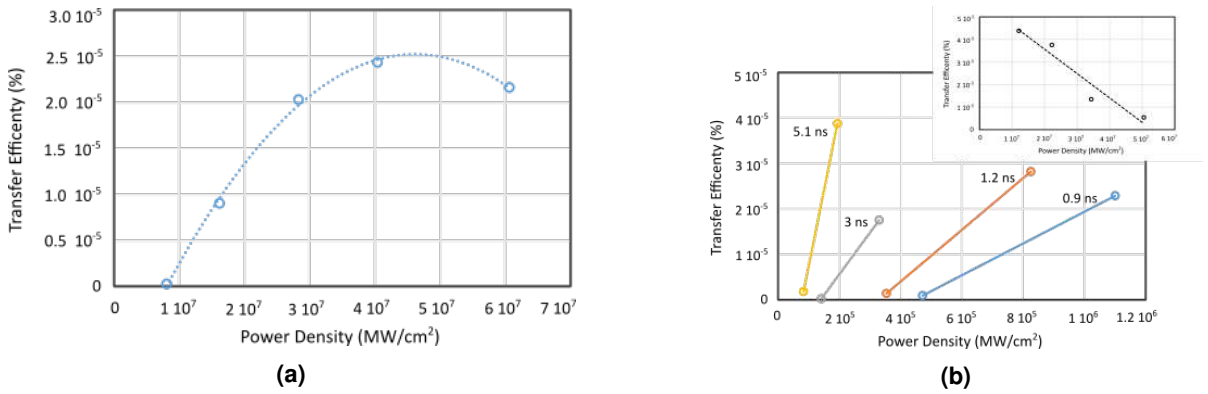

Figure 3. Kinetic energy transfer efficiency variation on pulse energy for (a) 35 fs pulse duration and (b) different pulse duration within ps range. (Inset: efficiency transfer slope variation at different laser power densities for same pulse energy variations)

an optimal transfer efficiency trend close to 0.001% for $I_0 \approx 500$ GW/cm^2 power densities, corresponding to a pulse energy $W_p \approx 200$ mJ pulse energy and several ps pulse duration.

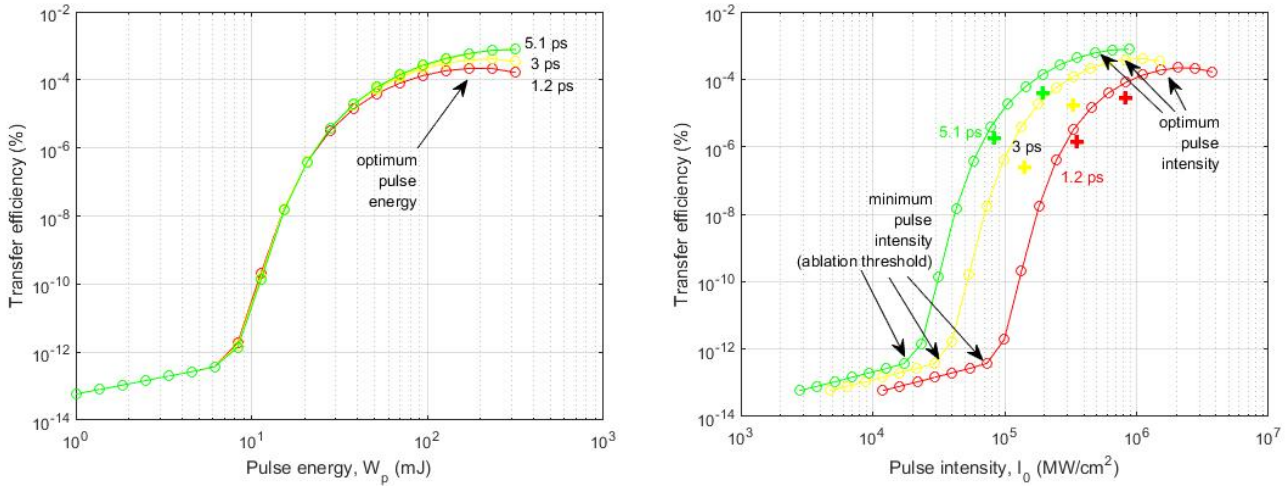

Figure 4. Transfer efficiency variation on (a) pulse energy $W_p = 200$ mJ and (b) pulse power density I_0 represented for different pulse durations $\tau = 1.2$ ps, 3 ps and 5.1 ps; the experimental data from Figure 3b were included as red ($\tau = 1.2$ ps), yellow ($\tau = 3$ ps), and green ($\tau = 5.1$ ps) crosses.

Multi-pulse regime

While single-pulse energy transfer efficiency is fundamentally important, for real (macroscopic) applications, it is very unlikely to be effective since the transferred energy is still relatively low from the macroscopic object's point of view, so, it is realistic to consider that trains of pulses should rather be used. In the following experiments, we have studied the influence of certain train parameters on transfer efficiency, such as number of pulses, repetition frequency, and train energy.

Multi-pulse regime: influence of the number of pulses and frequency

Considering the single-pulse kinetic energy transfer optimization, there is a tendency for intuitive extrapolation of the results for a multi-pulse regime. Measurements of transfer efficiency dependence of the number of train pulses using constant beam parameters (in other words by simply increasing train duration) are presented in Figure 5. From the energetic point of view, the result of pulse number increase will be an increase of the train energy (at constant pulse energy) and the experimental trend looks similar to the single-pulse in terms of energy grow influence. Thus, there will be an increase of the efficiency with the

number of pulses (and consequently with the train energy), but this increase will tend to reach a maximal value, after which, further increase of the number of pulses will start to decrease the global transfer efficiency. In Figure 5 are presented curves of transfer efficiency dependence on the number of pulses, for several train frequencies at comparable pulse power densities (2 - 3 MW/cm^2). From Figure 5 it should be noticed that even if all the curves have a similar trend of variation with the number

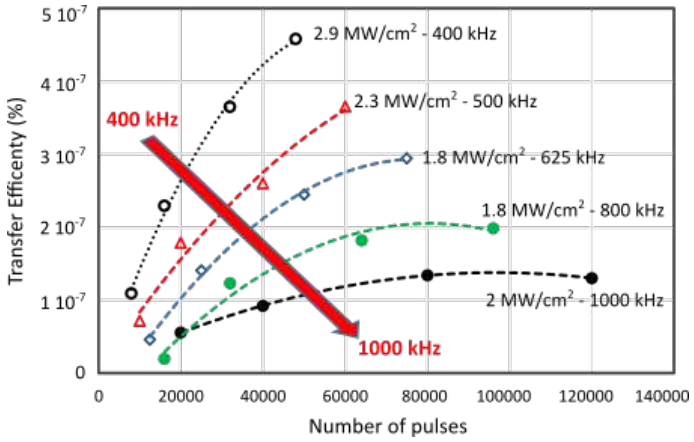

Figure 5. Experimental data on kinetic energy transfer efficiency variation with the number of pulses at different laser frequencies, for comparable power densities.

of pulses, their global amplitude variation is significantly influenced by the train frequency, rather than beam (instantaneous) power density. Thus, while further irradiating a titanium target with a 7 ps train pulses at 1064 nm we used constant average laser power (and respectively average power density). The influence of the train filling factor (respectively repetition rate) is effectively affecting the transferred impulse and respectively transfer efficiency (Figure 6) as expected. This could be easily understood by considering the decrease of the number of pulses in a given train duration and respectively the decrease of the effective laser-matter interaction time. Such reduction of the duration means an increase in the instantaneous power density of the pulses. For pulse duration of 7 ps and trains energies of hundreds of mJ, (instantaneous) power density should still be below the ablation threshold of the titanium, and an increase of the power density should correspond to a quasi-linear increase of the transfer efficiency as previously presented.

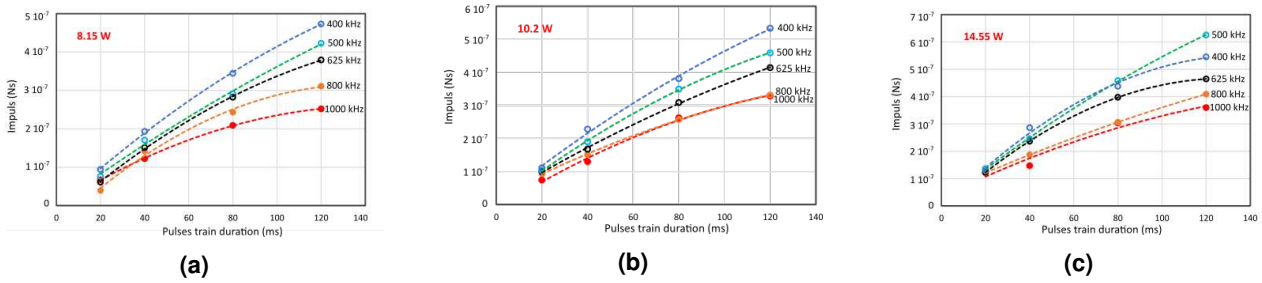

Figure 6. Frequency influence on impulse transfer for different average powers P_{train}: (a) 8.15 W, (b) 20.2 W and (c) 14.55 W average powers

By simulating transfer efficiency vs pulse number N for the multi-pulse regime, at different pulse energies and frequencies, obtained numerical results indicate that maintaining a constant pulse energy $W_p = W_{train}/N$, the peak temperature increases with the number of pulses during multi-pulse irradiation. However, we should mention that, because of the computer resource limitations, we opted for simulating trains with higher energy per pulse (for limiting the number of pulses per train), so further presented simulations will have just a qualitative relevance for our experiments. Thus, Figure 7a presents the increase of surface peak temperature with pulse number, considering a 4 mJ pulse energy and a succession period between two consecutive pulses $\tau_{int} = 100\ \tau$. In these conditions, the boiling temperature at the surface is reached after just 10 pulses. For comparison, simulations were also carried with the same pulse energy and pulse number conditions, considering that the target is cooled down to the original temperature (300 K) before each pulse. The blue curve (straight line) in Figure 7a indicates that the peak temperature is constant when increasing the pulse number and does not reach the melting or boiling points during multi-pulse irradiation. In Figure 7b a strong increase of the kinetic energy transfer efficiency of 4 mJ pulses is obtained after just 10 pulses.

Numerical results indicate that, even if the first pulses do not produce ablation of the target, after a certain number of laser pulses, the peak temperature of the surface increases above the material boiling values and initiates ablation processes, further leading to a significant increase of the transfer efficiency. For comparison, the blue curve (flat curve) was calculated considering that the target is cooled down to the original temperature before each pulse. The inset plot in Figure 7b demonstrates a linear increase of the efficiency with pulse number when cumulative heating of the target is not accounted for. For simulating a train of pulses with twice repetition frequency (2 f_p) of the same laser average power, we set twice more pulses in the irradiation time train at half pulse energy W_p and half the integration time. Numerical simulations from Figure 7c are representing the transfer efficiency dependence on the number of pulses at three frequencies:f_p, $2f_p$ and $3f_p$.

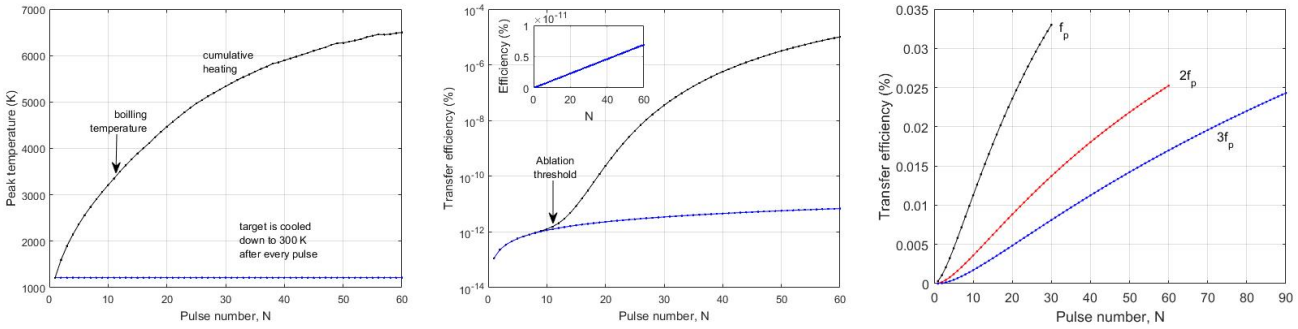

Figure 7. (a) Surface peak temperature vs pulse number. (b) Transfer efficiency vs pulse number. The blue curve and the inset plot correspond to 'cooled' targets down to (300 K) before each consecutive pulse. (c) Transfer efficiency vs pulse number at three working frequencies.

To clarify the origin of the efficiency dependence on frequency, we carried out calculations to determine the dependence of transfer efficiency on pulse number and train duration. For that, we considered that during the fixed train duration τ_{train}, there are generated N = 30, 60, and 90 pulses at a succession period between two consecutive pulses τ_{int} of 200τ, 100τ, and 70τ, respectively, corresponding to three different repetition frequencies $f_p = 1/\tau_{int} = N/\tau_{train}$: f_p, $2f_p$ and $3f_p$ respectively. First, we neglected the heat accumulation between consecutive pulses (Figure 8a), and secondly, we accounted for the heat accumulation between consecutive pulses (Figure 8b). The results presented in Figure 8a indicate that the time interval between the pulses does not influence the transfer efficiency if we neglect the thermal energy accumulation from pulse to pulse. Figure 8b demonstrates that, when considering thermal energy accumulation at the same laser energy and pulse number, the efficiency increases up to 8 orders of magnitude when ablation initiates. Figure 8b also demonstrates that, when considering thermal energy accumulation, low repetition frequency pulses are several times more efficient in transferring their energy to the target as compared to the high repetition frequency pulses.

Multi-pulse regime: train energy influence

Power density increase by increasing the pulse energy $W_p = W_{train}/N$ in a train was investigated at different laser frequencies. Figure 9 indicates that for a given pulse-train duration and number of pulses N, the increase of the train energy W_{train} is inducing an increase of the global transfer efficiency. However, the increase of the energy is producing a smaller and smaller increase particularly with the decrease of the laser-matter interaction duration (which is pulse duration multiplied by the 'number of pulses') and respectively the increase of the power density. As can be seen in Figure 9a, for a 20 ms train duration, the increase of the power density , is producing a smaller and smaller transfer efficiency increase, regardless if it was obtained by shortening the laser-matter interaction time (decrease of the number of pulses) or by further increasing pulse energy. In the inset of Figure 7 is presented the slope variation trend on the power density, for different frequencies (number of pulses) in the train with 20 ms duration. From an application point of view, if for a single pulse this corresponds in our case to an about 500:1 power density ratio with the ablation threshold, in the case of the multi-pulse regime, it should correspond to an optimal amount of ablated particles, generated by the train pulses in the given experimental conditions. The numerical results obtained in the multi-pulse regime on the dependence of transfer efficiency on the laser peak power density are presented in Figure 9b. We simulated two different repetition frequencies, f_p and $2f_p$, considering that the total energy of the pulse train is divided to N = 10 and N = 20 pulses, respectively. Here, the total energy of the pulse train W_{train} is varied in the range 0.15-2 J, resulting in a pulse energy W_p = 15-200 mJ/pulse when N = 10, and 7.5-100 mJ/pulse when N = 20.

Similar experimental results were obtained for other different train durations as well, and comparative results for train durations of train 20 ms, 40 ms, 80 ms, and 120 ms, train energies W_{train} of several hundreds of mJ and different pulse

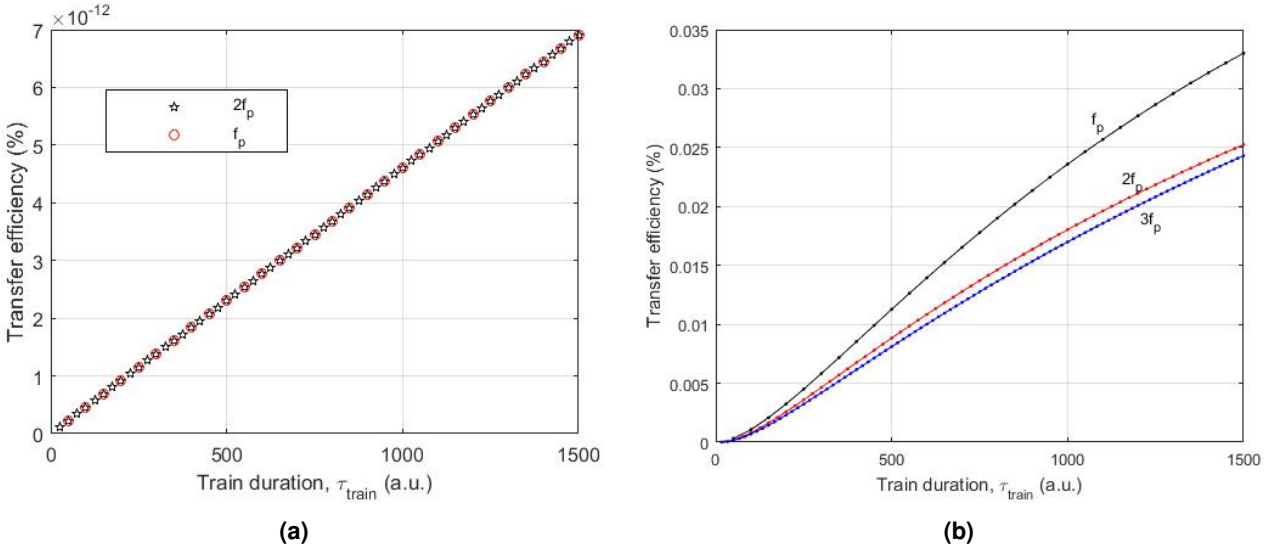

Figure 8. The transfer efficiency vs train duration. (a) by neglecting the heat accumulation between pulses and (b) by accounting for the heat accumulation between two consecutive pulses

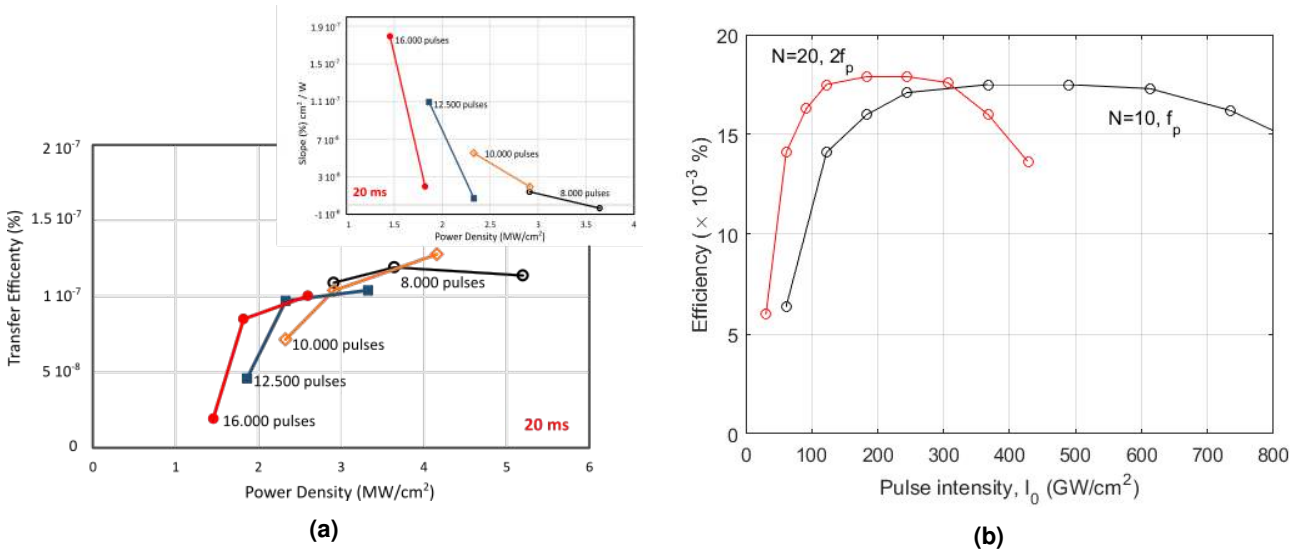

Figure 9. (a) Power density influence on kinetic energy transfer efficiency for 20 ms trains of 7 ps pulses (1064 nm), inset: power density influence on slope variation. (b) Numerical results on the dependence of transfer efficiency on the pulse power density.

frequencies f_p are presented in Figure 10. It could be observed that an increase in train energy is producing in all cases an increase of the kinetic energy transfer efficiency. However, at shorter train duration, the saturation of the transfer efficiency increase occurs at smaller energies, while for power densities around 5 MW/cm^2 further increase of train energy is already inducing a decreasing trend in the transfer efficiency variation after several tens of ms train duration, corresponding in our experimental cases to tens of thousands of pulses. Considering the hypothesis of the simulations and their correspondence with the experimental results we could draw some conclusions on the optimal number of pulses per train. That specific number should correspond to optimal ablation conditions which in our approximations rely on reaching a specific target surface temperature dependent on the heat accumulation process, a comparable amount of heat in the same time interval would be obtained by a double number of pulses of half energy. In other words, for a double operating frequency, the optimal energy transfer should correspond to a double number of pulses with a half-power density. Thus, considering the heat accumulation into the target as the dominant factor in initiating the ablation process, and consequently, as kinetic energy transfer buster

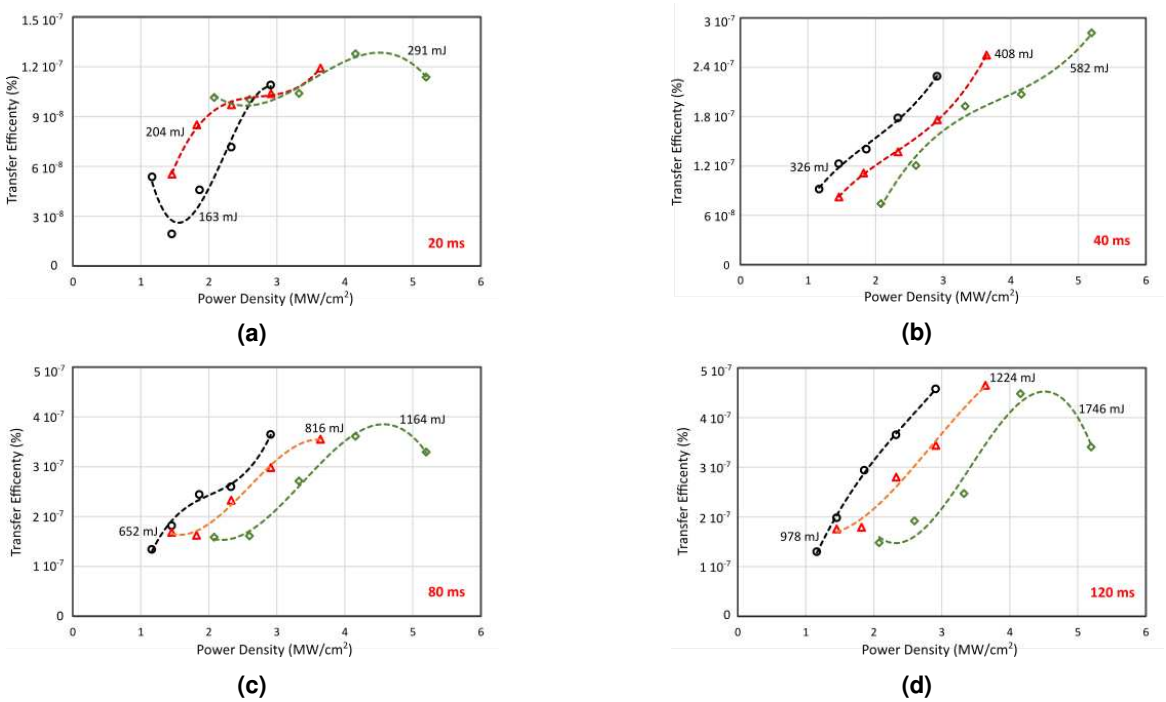

Figure 10. Kinetic energy transfer efficiency variation on power density for different train energy at (a) 20 ms, (b) 40 ms, (c) 80 ms and (d) 120 ms train duration

process, a generic variation formula of the optimal number of pulses per train dependence on train frequency and train energy should be given by:

$$N_{optimum} = k_p \frac{f_p}{W_{train}} \tag{1}$$

where f_p is the train repetition frequency, W_{train} is the train energy and k_p is a proportionality constant depending on the ablation process parameters, such as laser wavelength, pulse duration, material absorption coefficient at the laser wavelength and respectively ablation threshold for the specific wavelength and pulse duration, heat conductivity of the target material.

From an application point of view, this limitation of the transfer efficiency has clear importance. Thus, for a given (laser) pulse duration there is an optimal pulse energy and respectively an optimal number of pulses (in correlation with laser frequency) for an optimal transfer efficiency, after which the efficiency of the injected energy will start decreasing. In other words, transfer efficiency will increase with the total number of pulses and their energy, but, after a certain point, supplementary injected energy influence becomes neglectable or even start diminishing transferred kinetic energy global efficiency.

Methods

Experimental setup

An inertial pendulum can be considered one of the most reliable methods with sufficient sensitivity to characterize the impulse transferred from a light pulse to a macroscopic target. Following this approach, we built a pendulum with the length l_{pen} = 120 mm and a metallic foil target with 10 mm^2 area.

To minimize the errors generated from the air-target friction, the system was placed inside a low vacuum chamber as presented in Figure 11a where the pressure was set to ($\approx$ 0.1 mbar) during experiments that were all performed at room temperature. During experiments, the target was irradiated with two types of lasers: a high repetition rate "Lumera" Nd-YAG laser, tunable in the range (400 kHz - 1 MHz), delivering laser pulses with fixed pulse duration $\tau \approx 7$ ps at 1064 nm central wavelength with a high repetition rate f_p and a high power laser system (TEWALAS) delivering ultrashort pulses with a tunable duration from tens of picoseconds (ps) down to 25 femtoseconds (fs) at λ_0 = 800 nm central wavelength and 10 Hz maximum repetition rate. The laser beam spot area on target from both lasers was $A_{spot} \approx 7$ mm^2. In this experimental configuration, the laser pulses hit the target inducing oscillation along a direction parallel with the laser beam. The target position was recorded using a CCD camera (Basler GigE) placed perpendicular to the pendulum's oscillation direction with a fixed frame rate.

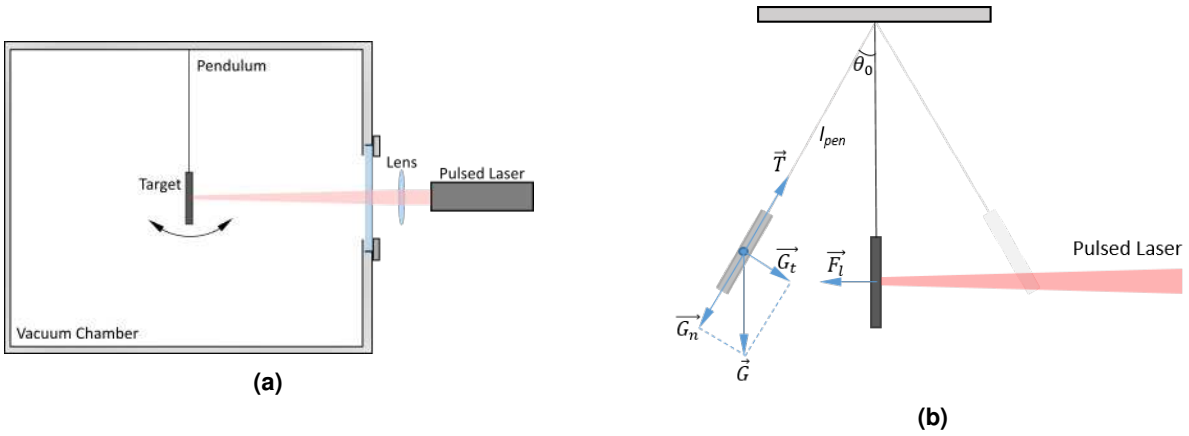

Figure 11. (a) Experimental setup of gravitational pendulum and (b) schematic forces diagram

Within our experimental approach, by knowing the laser pulse energy W_p, experimentally measured using a standard pyroelectric energy meter, and by measuring the pendulum kinetic energy E_{kin} we could evaluate energy transfer efficiency. By knowing the target mass $m \approx 25$ mg and pendulum length l_{pen}, from pendulum deviation d_p formula:

$$\theta = tan^{-1}\left(\frac{d_p}{l_{pen}}\right) \tag{2}$$

and the target maximal height h as represented in Figure 11b:

$$h = l_{pen}(1 - cos(\theta)) \tag{3}$$

and by further considering energy conservation between potential E_p and kinetic E_{kin}, maximal energies:

$$E_{p,max} = E_{kin,max} => h \cdot m \cdot g = \frac{1}{2} m \cdot v^2 \tag{4}$$

where v is the target velocity and g gravitational acceleration constant, we could evaluate the transferred kinetic energy and respectively kinetic energy transfer efficiency T_{ef} as follows:

$$T_{ef}(\%) = \frac{E_{kin,max}}{W_p} \times 100. \tag{5}$$

Theoretical modeling and preliminary calculations

We have considered that above a specific threshold of laser power density, the laser-target interaction leads to ablation as a thermally activated process. The ablation is initiated by the absorption of the laser energy by the free electrons via inverse Bremsstrahlung[16], followed by rapid picosecond scale relaxation of the energy via electron-electron and electron-phonon collisions. The thermal penetration depth is $l_T = \sqrt{2D\tau}$, where D is the thermal diffusivity of the target and τ is the laser pulse duration. Accounting for the pulse duration involved in this study (mostly ps regimes), the thermal penetration depth is of the order of 5μm ÷ 5 nm, which is very small as compared to the laser beam diameter d = 3 mm on the target surface. Thus, the temperature distribution in the axial z-direction can be determined from the 1D heat equation[11–14,17]:

$$\rho c_p \frac{\partial T}{\partial t} - k\frac{\partial^2 T}{\partial z^2} = S. \tag{6}$$

Here, ρ, c_p, and k denote the mass density, the specific heat, and the thermal conductivity of Titanium, respectively, taken as constant parameters. The source term of the heat equation describes the volumetric laser energy input near the irradiated surface:

$$S(z,t) = (1-R)\alpha I(t) e^{-\alpha z} e^{-\alpha_p l_p} \tag{7}$$

where, the surface reflectivity R = 0.61 and the optical absorption coefficient of the target, $\alpha = 2.36 \cdot 10^7$ cm^{-1} were calculated from complex refractive index database[18].

For a Gaussian laser beam, the power density profile is described by:

$$I(t) = I_0 \exp\left[-4ln2\frac{(t-t_0)^2}{\tau^2}\right] \tag{8}$$

where τ is the pulse duration at FWHM. The peak power density I_0 was calculated so that by time integration of the power density $I(t)$ function and multiplication to the laser spot area (≈ 7 mm^2) to obtain the experimentally measured pulse energy.

Depending on the laser power density, the vapor plume ionizes. Here we account for a power density dependent ionization degree of the plasma η, with a maximum ionization of 6% at the highest power density. The length of the plasma plume l_p is considered directly related to the pulse duration, the minimum length accounted here being 50 nm, which is approximately the distance of propagation of the plasma plume during 1 ps. The absorption coefficient of the plasma α_p (cm^{-1}) through inverse Bremsstrahlung is given by[11,13–15]:

$$\alpha_p = 1.37 \cdot 10^{-35}\lambda^3 n^2 T_p^{-1/2}\left(1 - e^{-\frac{h_{Planck}c}{\lambda k_B T_p}}\right) \tag{9}$$

where, k_B is the Boltzmann constant, n is the plasma density and T_p is the plasma temperature. An exponential decay (Beer-law like) function describes the attenuation of the laser beam within the absorbing plasma plume that expands away from the target, as indicated in Equation 7. The expanding plasma plume exerts a recoil pressure,

$$P_{rec} \approx 0.56 P_{sat} \tag{10}$$

(which is a fraction of the saturated vapor pressure P_{sat}), on the target surface. The saturated vapor pressure, plasma temperature and plasma density are considered dependent on the temperature of the target surface[11,14,15].

The boundary and initial conditions of the heat equation are as follows: the initial condition at the beginning of the laser pulse is

$$T_{z,t=0} = 300K \tag{11}$$

A constant-temperature boundary condition is set at rear surface located at $z = 100l_T$:

$$T_{z=100l_T,t} = 300K. \tag{12}$$

The boundary condition giving the energy balance at the irradiated surface (z = 0), writes

$$-k\frac{\partial T}{\partial z}(z=0,t) = \rho v_{ev}(\lambda_{vap} + \lambda_{boil}) \tag{13}$$

where v_{ev} is surface receding velocity due to evaporation, λ_{vap} and λ_{boil} represent the latent heats, of melting and vaporization, respectively. The heat equation 6 was solved numerically in MATLAB. For every laser pulse, the integration time for the heat equation was set to about 100 τ, with a minimum time step of 20 fs. The spatial computational domain was set to a total thickness $h = 100l_T$, with much denser mesh near the front surface (i.e. smaller than 0.1 nm) to accommodate the volumetric laser absorption at this surface.

We calculated numerically the temperature of the target surface see Figure 12a for example, and the corresponding recoil pressure P_{rec} given by equation 10 of the expanding vapor, as a function of time. The recoil pressure P_{rec} and the laser pressure:

$$P_{rad} = (1+R)I/c \tag{14}$$

were added to determine the total pressure exerted on the Titanium target: $P_{tot} = P_{rad} + P_{rec}$. Figure 12b presents the dependence of total pressure P_{tot} exerted on the target surface on laser power density, which is varied by changing the pulse energy at constant pulse duration $\tau = 5.1$ ps. One can note that, above the ablation threshold power density $I_{th} \approx 20$ GW/cm^2, the recoil pressure due to ablation P_{rec} has the main contribution on the total pressure, being up to 4 orders of magnitude higher than the radiation pressure P_{rad}, as also other studies predicted[4].

By multiplying the total pressure P_{tot} to the laser beam spot area on the target surface ($A_{spot} \approx 7$ mm^2), we determined the time-dependent total force exerted on the target surface. By time integration of the force, the momentum transferred to the target by one pulse was determined:

$$p = A_{spot}\int_0^{100\tau} P_{tot}(t)dt. \tag{15}$$

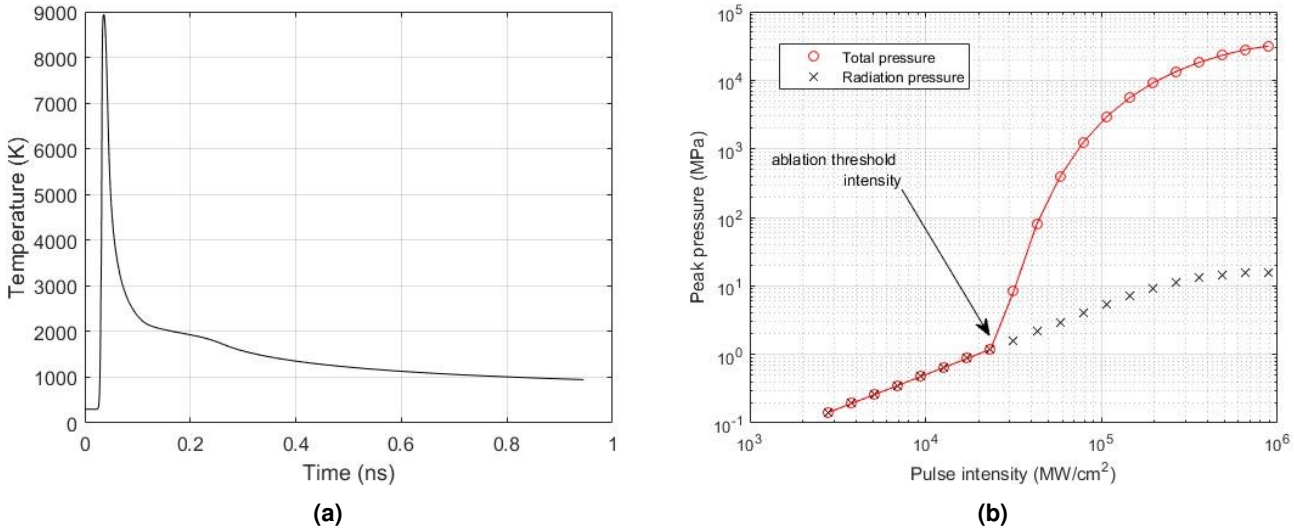

(a) (b)

Figure 12. Simulation results of (a) target-surface temperature time dependence for 800 nm, τ = 7 ps and 10 mJ pulse and b) peak pressure dependence on laser pulse peak power density I_0 at λ= 800 nm and τ = 5.1 ps pulses

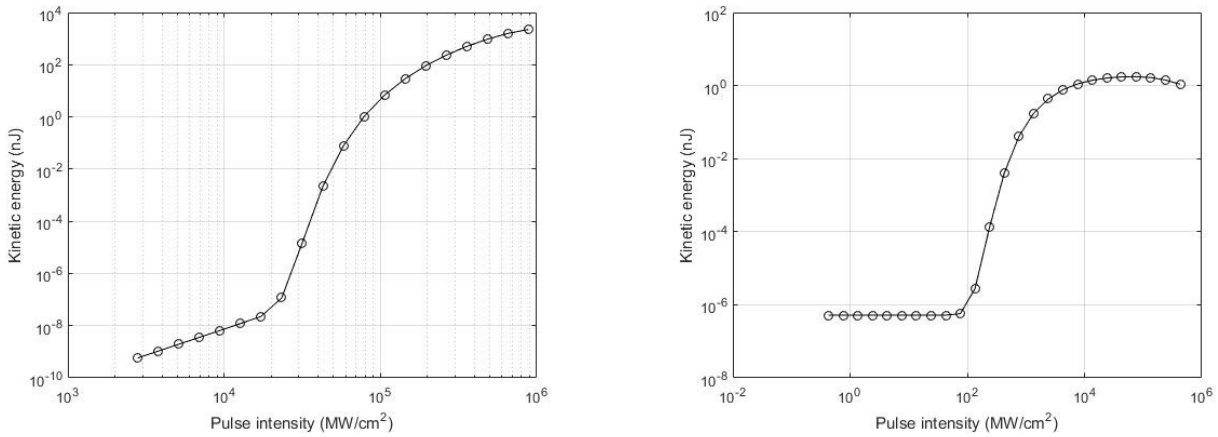

(a) (b)

Figure 13. Kinetic energy E_{kin} dependence on power density, controlled by: (a) pulse energy W_p between 1-300 mJ, λ =1064 nm, τ = 5.1 ps; (b) pulse duration τ between 1 μs ÷ 1 ps for constant pulse energy W_p = 30 mJ

Then, the kinetic energy of the target was derived as $E_{kin} = p^2/2m_{target}$ and, by dividing the kinetic energy by the total energy of the laser pulses, we determined the efficiency of the energy transfer. In Figure 13a the peak power density is varied by changing the pulse energy in the range 1 - 300 mJ while pulse duration is kept constant at 5.1 ps. In Figure 13b the peak power density is varied by changing the pulse duration in the range 1 μs - 1 ps while pulse energy is kept constant at 30 mJ.

In the multi-pulse regime, the simulations were carried considering the spatial distribution of the temperature from the end of the integration time corresponding to a certain laser pulse as the initial condition for the next pulse. Additionally, we considered that the length of the vapor plume corresponding to a laser pulse is directly related to the pulse number N: as was also experimentally observed in previous work[19].

Conclusions

In conclusion, we could summarize that our experimental studies on an inertial pendulum with Ti targets combined with the theoretical simulations based on heat and photon energy transfer and respectively photon reflection have shown a kinetic energy transfer efficiency optimal value for beam power densities about 500 times bigger than the ablation threshold values,

corresponding in our case to an optimal pulse duration of tens to hundreds of ps. Consequently, the optimal pulse energy for given pulse duration and beam diameter is the energy providing a power density on the target that is 500 times higher than the ablation threshold. For the case of multi-pulse regimes, as a more effective approach from laser-thrust applications, there is a more efficient transfer from lower repetition rate train pulses, then higher rates. Increasing the train energy is in principle increasing transfer efficiency but within a limited variation range while the optimal number of pulses per train is depending proportionally on repetition rate and inverse proportionally on the beam power density (and respectively pulse energy). The proportionality constant is depending on the target material and other beam parameters. In our experimental case of the Ti target, 7 ps infrared laser pulse duration and μJ energies per pulse and repetition rates of hundreds of MHz, the optimal number of pulses is in the range of tens to few hundreds of thousands of pulses per train while the maximal transfer efficiency could reach values of 0.02%.

References

1. Zhao, X.-T., Tang, F., Han, B. & Ni, X.-W. The influence of laser ablation plume at different laser incidence angle on the impulse coupling coefficient with metal target. *J. Appl. Phys.* **120**, 213103, DOI: 10.1063/1.4971247 (2016).
2. Battocchio, P. *et al.* Ballistic measurements of laser ablation generated impulse. *Meas. Sci. Technol.* DOI: 10.1088/1361-6501/abace6 (2020).
3. D'Souza, B. & Ketsdever, A. Investigation of Laser-Surface Interactions Using a Nano-Impulse Balance. In *35th AIAA Plasmadynamics and Lasers Conference*, DOI: 10.2514/6.2004-2664 (American Institute of Aeronautics and Astronautics, 2004).
4. Kantrowitz, A. Propulsion to Orbit by Ground-Based Lasers. *Astronaut. Aeronaut.* **10**, 74 – 76 (1972).
5. Shui, V. H., Young, L. A. & Reilly, J. P. Impulse Transfer from Pulsed CO, Laser Irradiation at Reduced Ambient Pressures. *AIAA J.* **16**, 649–650, DOI: 10.2514/3.60953 (1978).
6. Esmiller, B., Jacquelard, C., Eckel, H.-A. & Wnuk, E. Space debris removal by ground-based lasers: main conclusions of the European project CLEANSPACE. *Appl. Opt.* **53**, I45–I54, DOI: 10.1364/AO.53.000I45 (2014).
7. Phipps, C. R. *et al.* Laser impulse coupling measurements at 400 fs and 80 ps using the luli facility at 1057 nm wavelength. *J. Appl. Phys.* **122**, 193103, DOI: 10.1063/1.4997196 (2017).
8. Kim, I. J. *et al.* Radiation pressure acceleration of protons to 93 mev with circularly polarized petawatt laser pulses. *Phys. Plasmas* **23**, 070701, DOI: 10.1063/1.4958654 (2016). Publisher: American Institute of Physics.
9. Esirkepov, T., Borghesi, M., Bulanov, S. V., Mourou, G. & Tajima, T. Highly Efficient Relativistic-Ion Generation in the Laser-Piston Regime. *Phys. Rev. Lett.* **92**, 175003, DOI: 10.1103/PhysRevLett.92.175003 (2004). Publisher: American Physical Society.
10. Harilal, S. S., Freeman, J. R., Diwakar, P. K. & Hassanein, A. Femtosecond Laser Ablation: Fundamentals and Applications. In Musazzi, S. & Perini, U. (eds.) *Laser-Induced Breakdown Spectroscopy: Theory and Applications*, Springer Series in Optical Sciences, 143–166, DOI: 10.1007/978-3-642-45085-3_6 (Springer, Berlin, Heidelberg, 2014).
11. Stafe, M. & Negutu, C. Real-Time Monitoring of the Pulsed Laser Ablation of Metals Using Ablation Plasma Spectroscopy. *Plasma Chem. Plasma Process.* **32**, 643–653, DOI: 10.1007/s11090-012-9359-y (2012).
12. Bulgakova, N. & Bulgakov, A. Pulsed laser ablation of solids: transition from normal vaporization to phase explosion. *Appl. Phys. A* **73**, 199–208, DOI: 10.1007/s003390000686 (2001).
13. Amoruso, S., Armenante, M., Berardi, V., Bruzzese, R. & Spinelli, N. Absorption and saturation mechanisms in aluminium laser ablated plasmas. *Appl. Phys. A* **65**, 265–271, DOI: 10.1007/s003390050577 (1997).
14. Stafe, M. Theoretical photo-thermo-hydrodynamic approach to the laser ablation of metals. *J. Appl. Phys.* **112**, 123112, DOI: 10.1063/1.4771692 (2012).
15. Stafe, M., Marcu, A. & Puscas, N. N. *Pulsed Laser Ablation of Solids: Basics, Theory and Applications* (Springer, New York, NY, 2013), 2014th edition edn.
16. Johnson, P. B. & Christy, R. W. Optical constants of transition metals: Ti, V, Cr, Mn, Fe, Co, Ni, and Pd. *Phys. Rev. B* **9**, 5056–5070, DOI: 10.1103/PhysRevB.9.5056 (1974). Publisher: American Physical Society.
17. Murray, T. W. & Wagner, J. W. Laser generation of acoustic waves in the ablative regime. *J. Appl. Phys.* **85**, 2031–2040, DOI: 10.1063/1.369498 (1999).
18. RefractiveIndex.INFO. Refractive Index database Element Titanium (https://refractiveindex.info/?shelf=main&book=Ti&page=Johnson).

19. Marcu, A., Stokker, F., Zamani, R. R., Lungu, C. P. & Grigoriu, C. High repetition rate laser ablation for vapor–liquid–solid nanowire growth. *Curr. Appl. Phys.* **14**, 614–620, DOI: 10.1016/j.cap.2014.02.002 (2014).

Acknowledgements

Experimental work was performed within the frame of the ROSA-STAR project 189/2017 while theoretical simulations were supported by ELI-RO with project number ELI_13/16.10.2020.

Author contributions statement

Marcu A. designed the experiments and wrote the manuscript's experimental part, Stafe M. performed modeling and simulations, and wrote the manuscript's theoretical part, Barbuta M. performed CCD data acquisition and processing as well as the design of the used processing algorithms, Ungureanu R. implemented fs laser experiment and performed it together with Serbanescu M., Calin B. performed ps laser experiments together with Barbuta M., while Puscas N. contributed to the data interpretation and correlation of the experimental and theoretical results. All authors reviewed the manuscript.

Additional information

Competing interests The authors declare no competing interests.

Figures

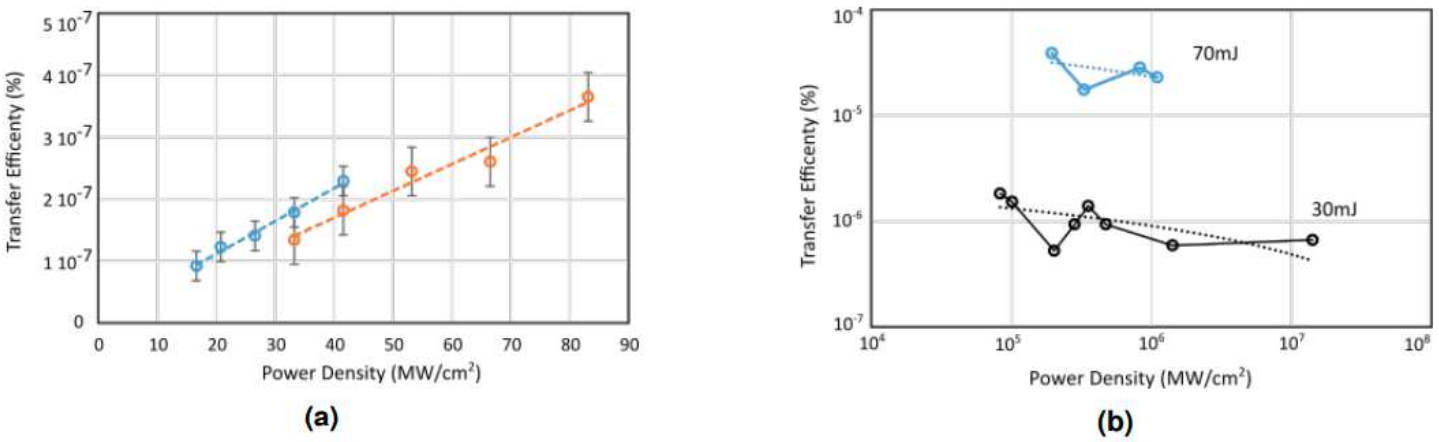

Figure 1

Please see the Manuscript PDF file for the complete figure caption

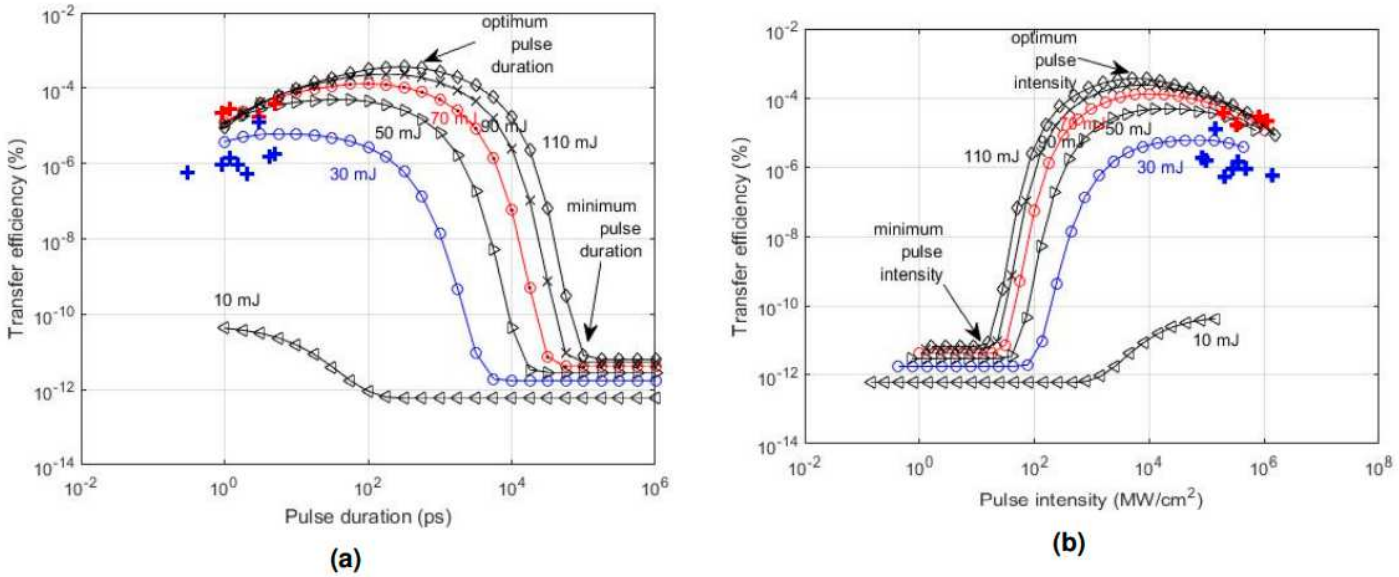

Figure 2

Please see the Manuscript PDF file for the complete figure caption

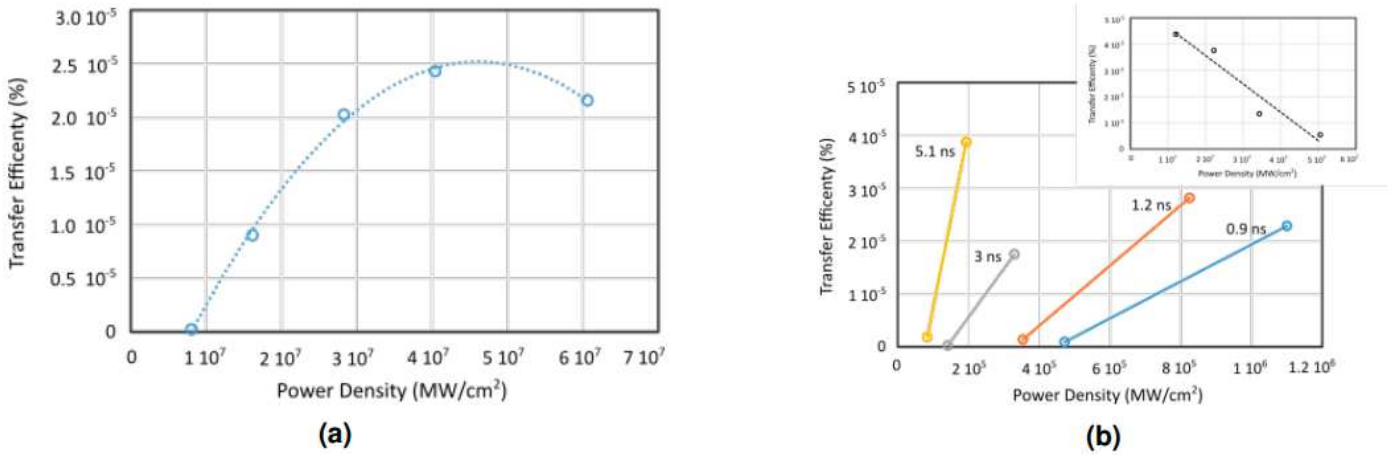

Figure 3

Please see the Manuscript PDF file for the complete figure caption

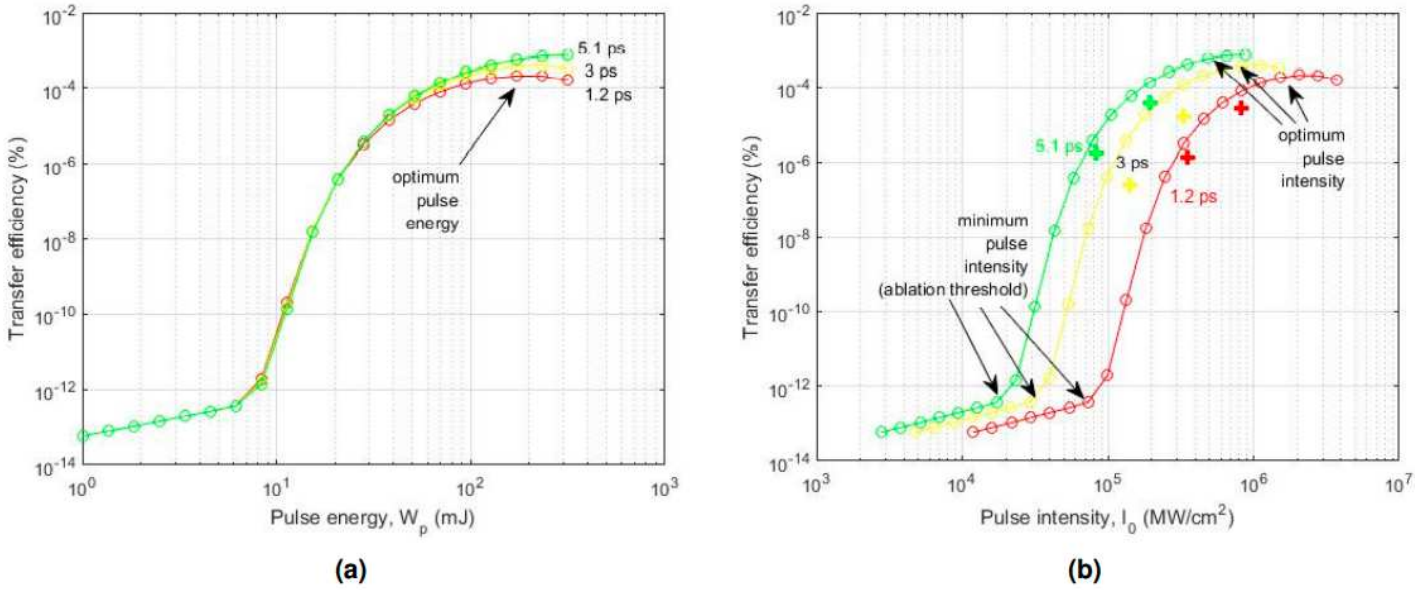

Figure 4

Please see the Manuscript PDF file for the complete figure caption

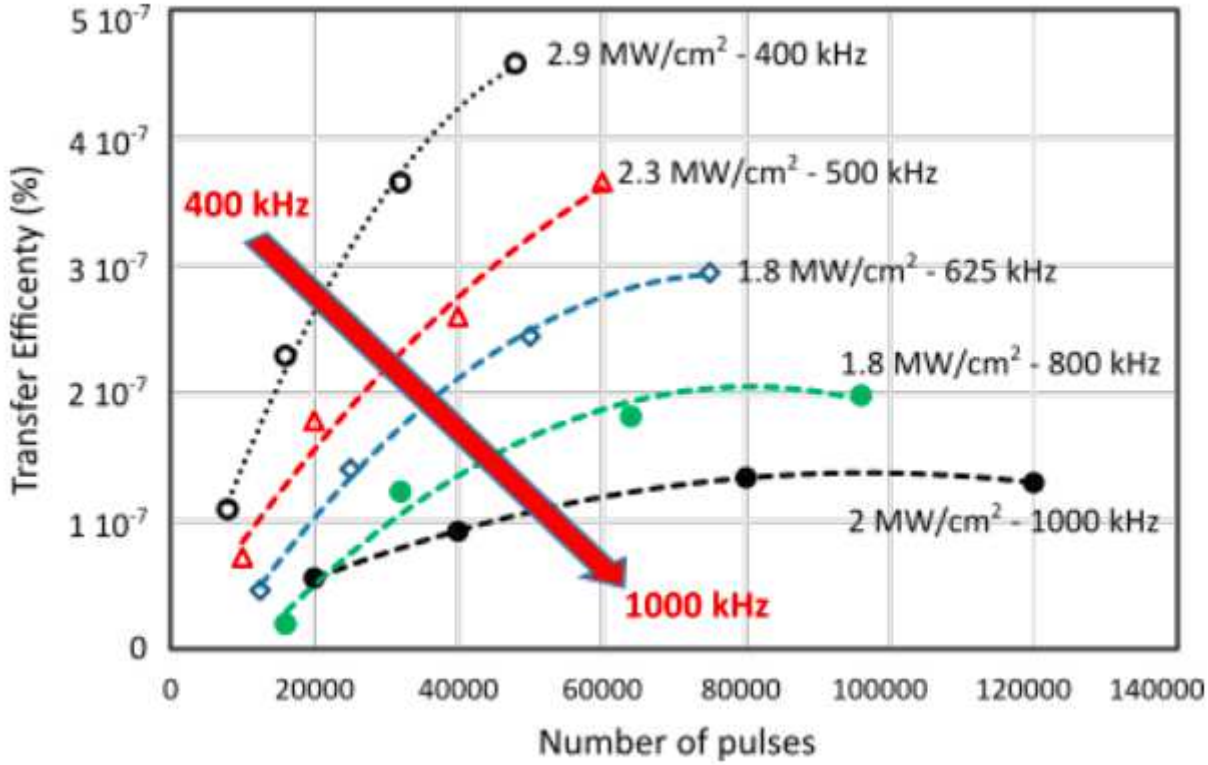

Figure 5

Please see the Manuscript PDF file for the complete figure caption

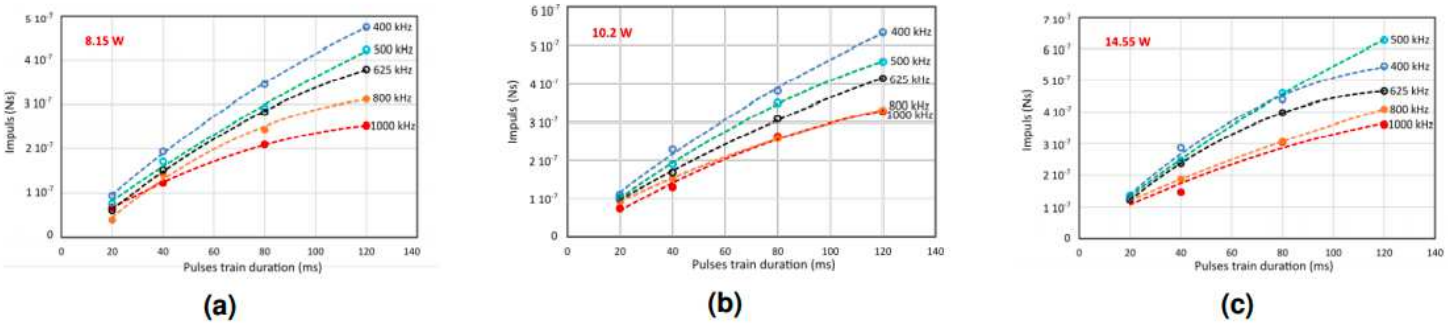

Figure 6

Please see the Manuscript PDF file for the complete figure caption

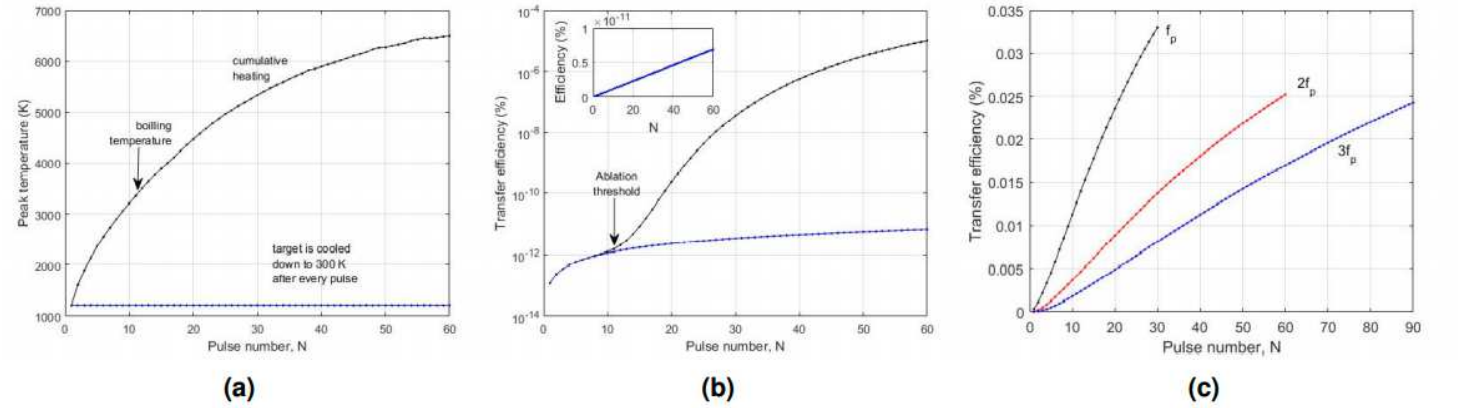

Figure 7

Please see the Manuscript PDF file for the complete figure caption

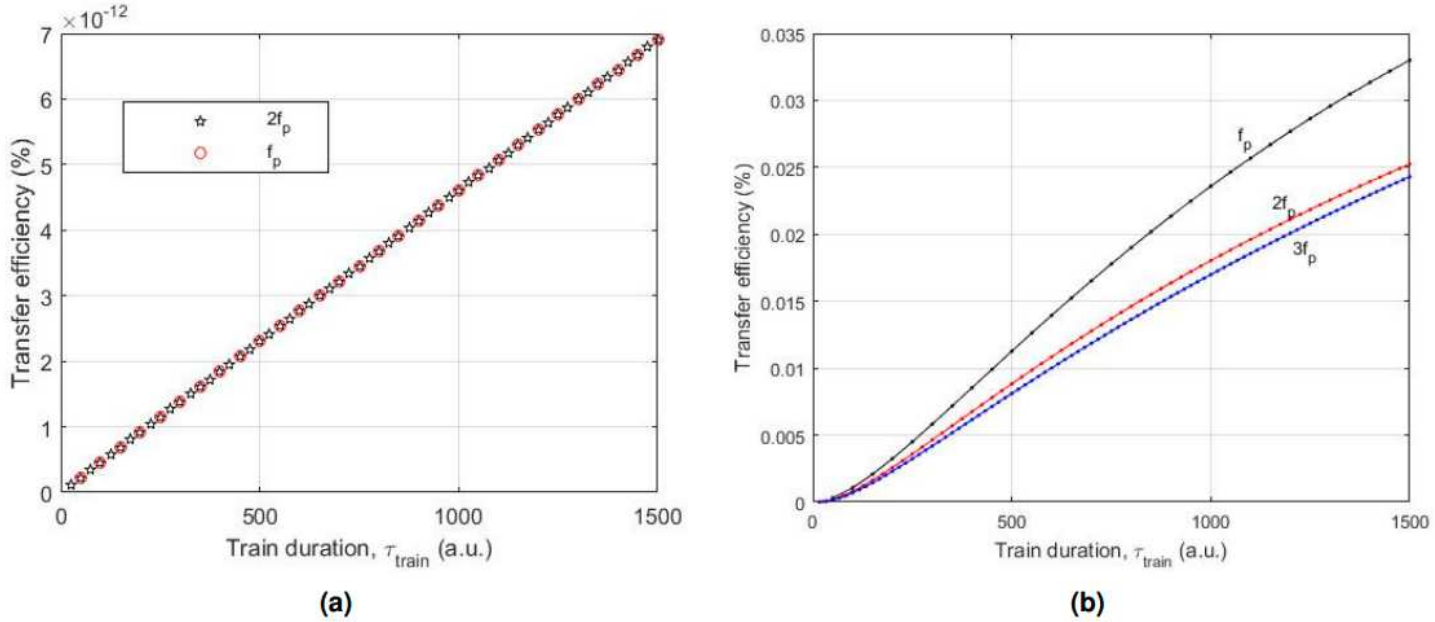

Figure 8

Please see the Manuscript PDF file for the complete figure caption

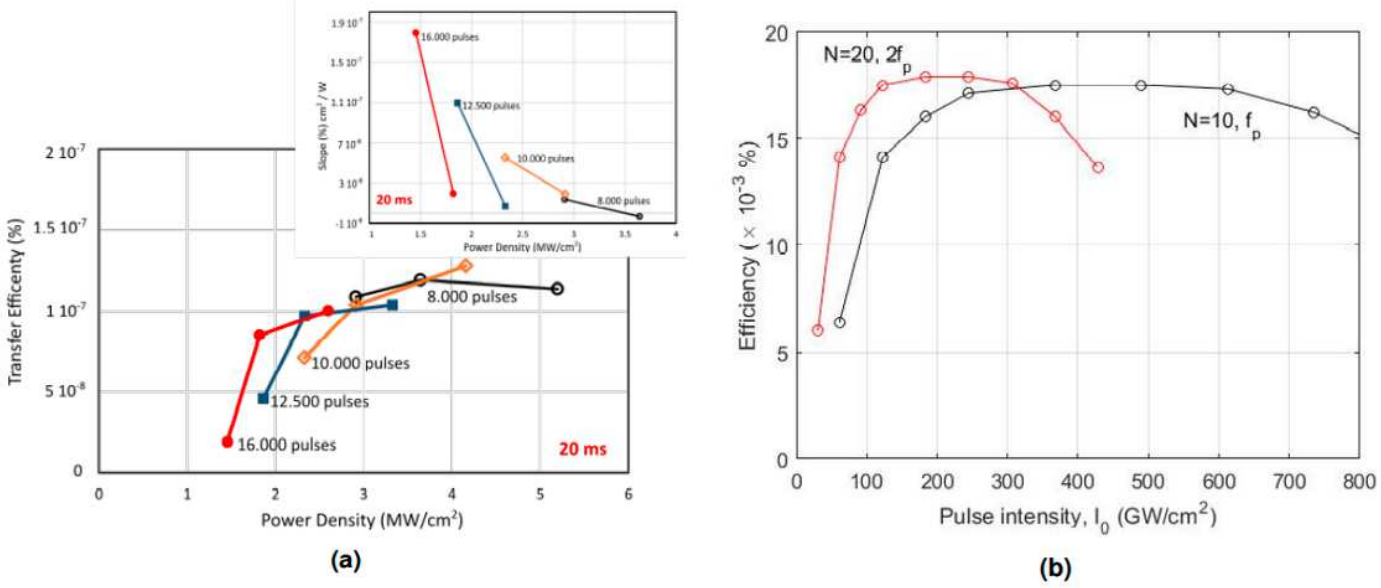

Figure 9

Please see the Manuscript PDF file for the complete figure caption

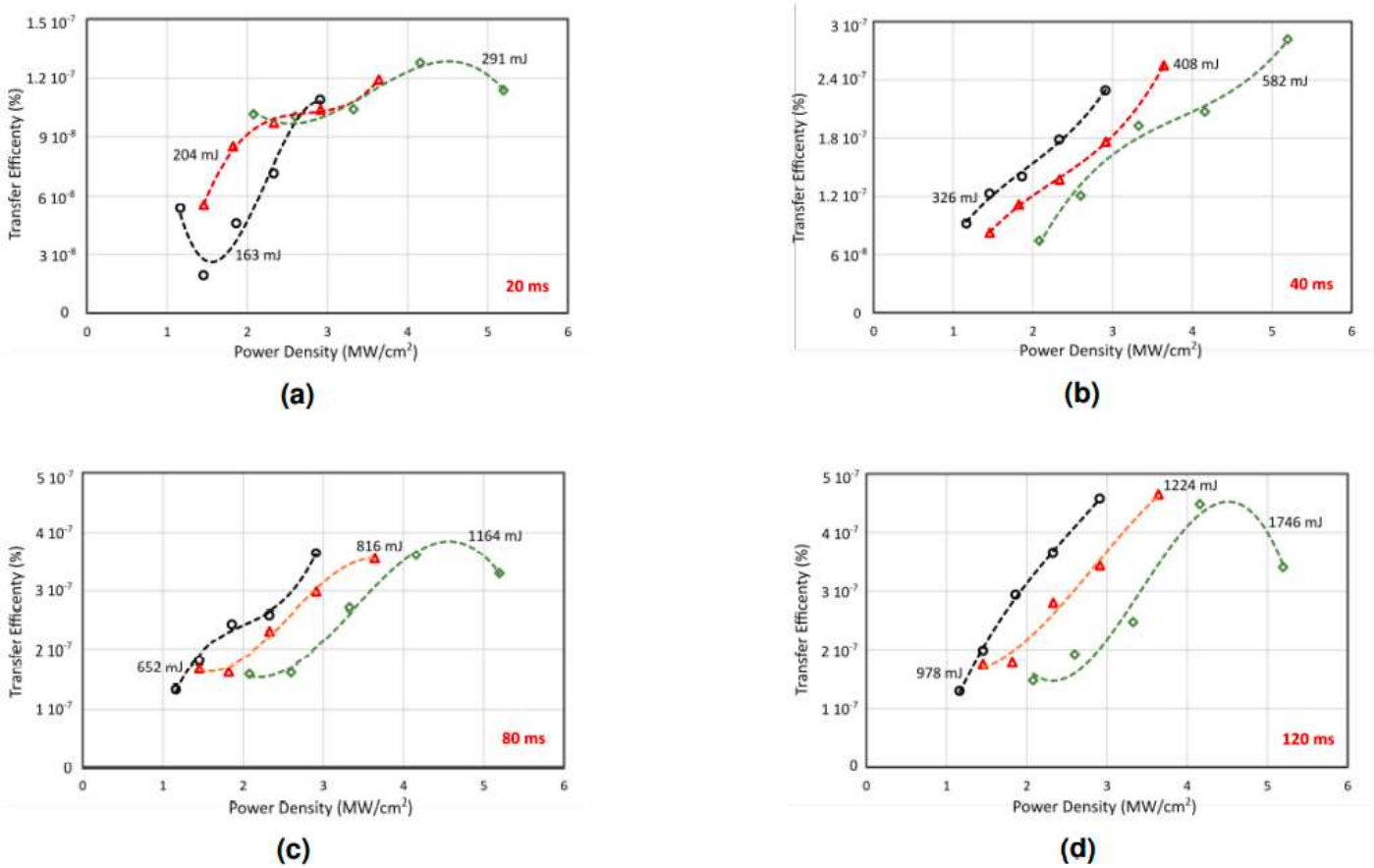

Figure 10

Please see the Manuscript PDF file for the complete figure caption

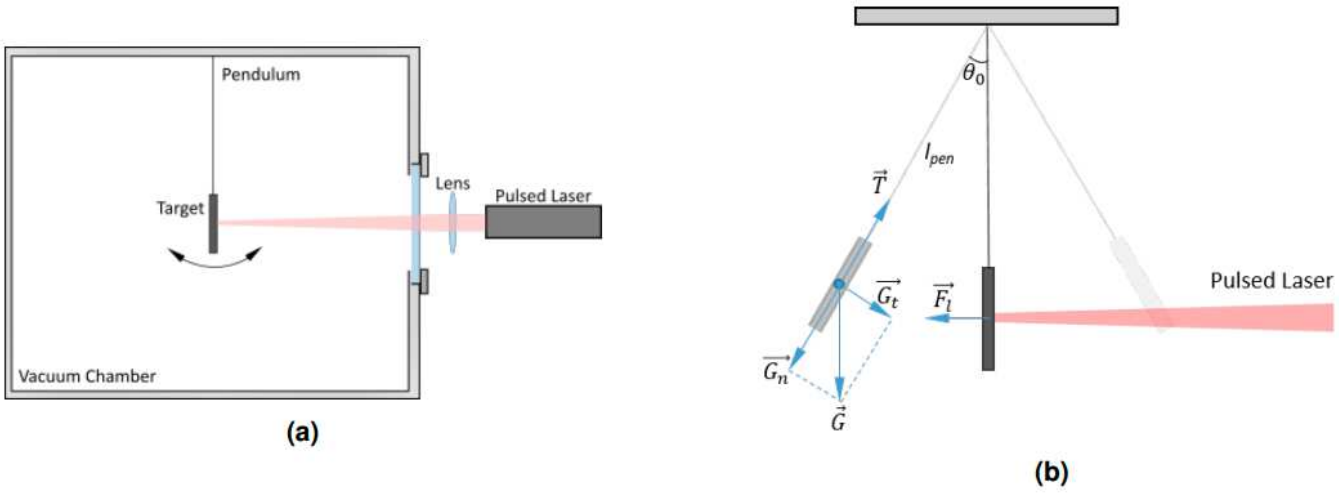

Figure 11

Please see the Manuscript PDF file for the complete figure caption

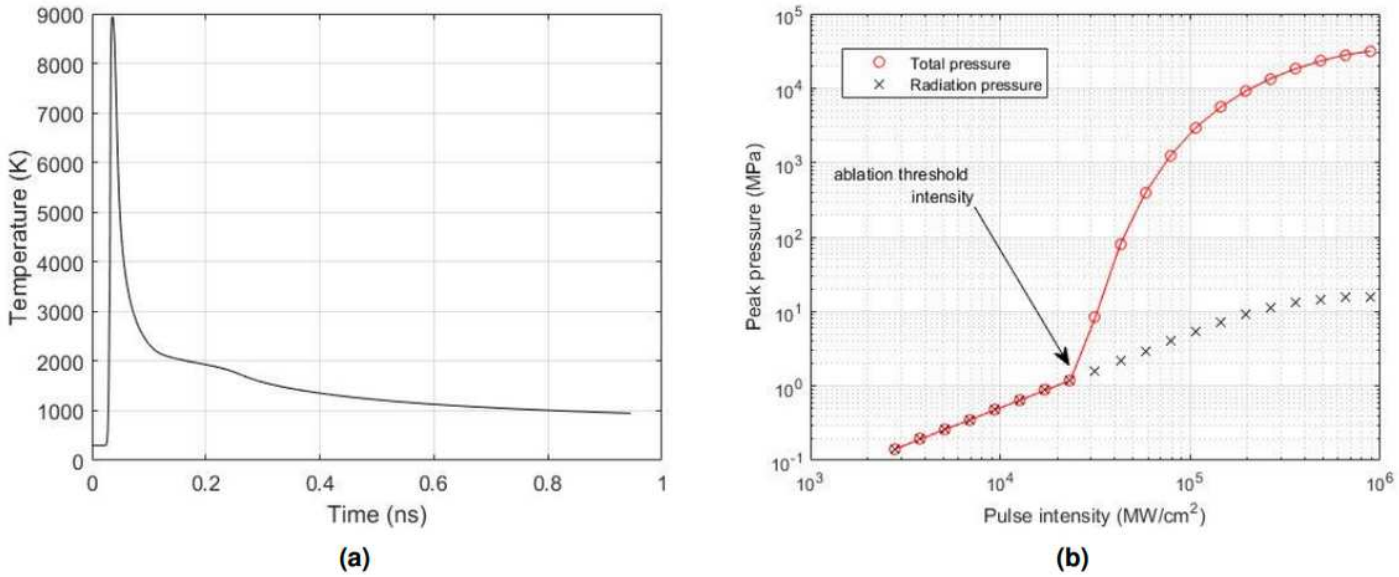

Figure 12

Please see the Manuscript PDF file for the complete figure caption

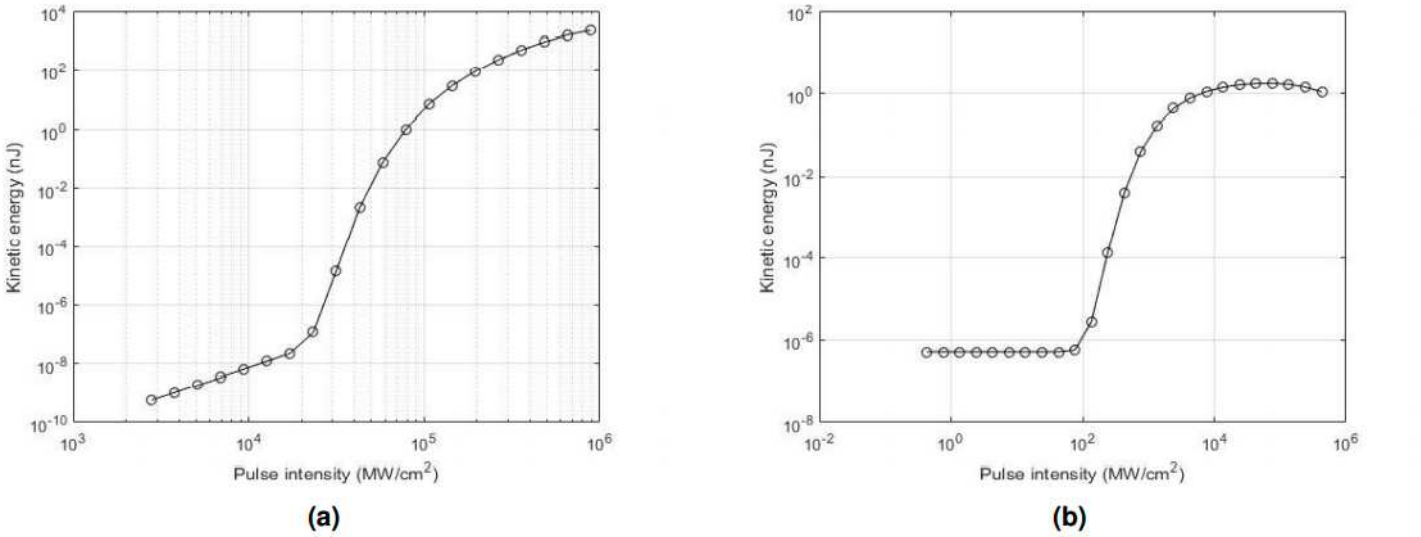

Figure 13

Please see the Manuscript PDF file for the complete figure caption